BACKHOE KINEMATICS & DYNAMICS

For use in the design of the Haptic Backhoe project

Joe Frankel

Georgia Institute of Technology

Intelligent Machines Dynamics Laboratory

August 20, 2003

CONTENTS

Abstract

This report is intended for use in the design of the *Robotic Backhoe with Haptic Display* project at the Intelligent Machine Dynamics Laboratory (IMDL) at Georgia Tech. The work herein describes the kinematic and dynamic relationships between the cylinder forces and resulting motions of the backhoe's four degrees of freedom, namely the swing, boom, stick, and bucket links. The geometric transformations between joint angles and cylinder positions are derived, and both forward and reverse displacement analyses are solved. A LaGrangian dynamic model is presented to compute link accelerations from actuator forces. Finally, a desired digging trajectory is defined, and the reverse kinematic equations are used for simulation. This report is intended to be used as a stepping stone for programming the controller and haptic user interface for the Robotic Backhoe with Haptic Display.

Figure 1 is a photo of the backhoe used for this project, before modifications.

Figure 1: John Deere Model 47 Backhoe

Component Definitions and Labeling Conventions

The backhoe can be modeled as a 4R (four revolute joint) hybrid serial-parallel mechanism, with the swing joint axis normal to the ground and the remaining three joint axes parallel to the ground. Figure 1 is a photo of the backhoe, and Figure 2 illustrates the component frames and joint angles as used throughout this report. Note that relevant points in the mechanism have been labeled with numbers O_1-O_4 for the joint axis origins and letters *A-H* for the remaining axes relevant to the analysis. When describing linear and angular dimensions, the following convention has been ascribed. All linear (scalar) dimensions are given as r_{xy}, where *x* and *y* are either the numeric or alphabetic joint labels, with numbers before letters, and arranged in ascending order. For example, the distance from point B to origin O_1 would be r_{1B}, etc. Angular quantities are given in the format θ_{xyz}, where *x, y*, and *z* are the three points describing the angle in the *counterclockwise* direction. For example, the angle between the lines $\overline{O_2O_3}$ and $\overline{EO_3}$ is given by θ_{23E}. See Figure 2.

Figure 2: Component Frames and Joint Angles

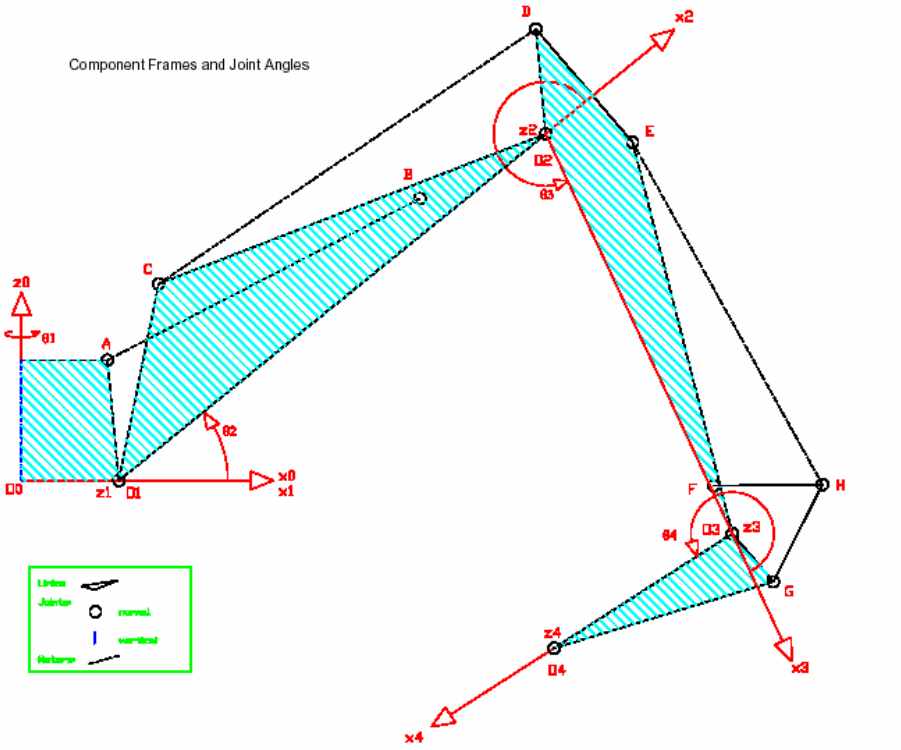

Scalar quantities are shown in italics. For example, the swing angle is given by θ_1. Vector and matrix quantities are shown in boldface format, with one-dimensional column vectors in lower case and two-dimensional matrices in uppercase. For example, $\boldsymbol{\theta} = [\theta_1 \quad \theta_2 \quad \theta_3 \quad \theta_4]^T$ indicates the four element joint angle vector and $\mathbf{M}$ is the 4x4 manipulator inertia matrix.

Position vectors are indicated in the format $\mathbf{p}_{xy}^{f}$, where the superscript *f* denotes the component frame and the subscript *xy* denotes the starting and ending points. For example, the notation $\mathbf{p}_{C3}^{2}$ denotes the position vector from point *C* to origin O_3 in component frame *2* (boom coordinates).

Cylinder lengths are denoted by the vector $\mathbf{y_c}$, where $y_c(i)$, $i=1:5$. Although the backhoe has four degrees of freedom, the swing link is associated with the first *two* cylinders, so $y_c(3)$ controls the boom, $y_c(4)$ the stick, and $y_c(5)$ the bucket. See Figure 2.

Some of the kinematic transformations make use of homogeneous transformation matrices and the geometric Jacobian. For these computations, the Denavit-Hartenberg labeling (DH) convention is used. The DH parameters for the backhoe are given in Table 1. The joint angles $\boldsymbol{\theta}$ uniquely determine the pose of the backhoe. The link lengths **a** and the twist angles $\boldsymbol{\alpha}$ are constants.

Table 1: Denavit-Hartenberg Parameters

Joint	Link Lengths $a(i)$	Joint Angles $\theta(i)$	Joint Offsets $d(i)$	Twist Angles $\alpha(i)$
1	a_1	θ_1	0	90°
2	a_2	θ_2	0	0
3	a_3	θ_3	0	0
4	a_4	θ_4	0	0

The bucket angle ϕ has been defined as the angle between the x_4 axis (bucket) and the x_0-y_0 plane, which is assumed to be parallel with the earth. The bucket angle is defined as positive downward as illustrated in Figure 3. This angle will be useful for describing the desired bucket trajectory in base frame coordinates.

Finally, subscripts and indices in parenthesis are used interchangeably in some cases. For example, $\theta_1 = \theta(1)$, etc.

Figure 3: Bucket Angle ϕ

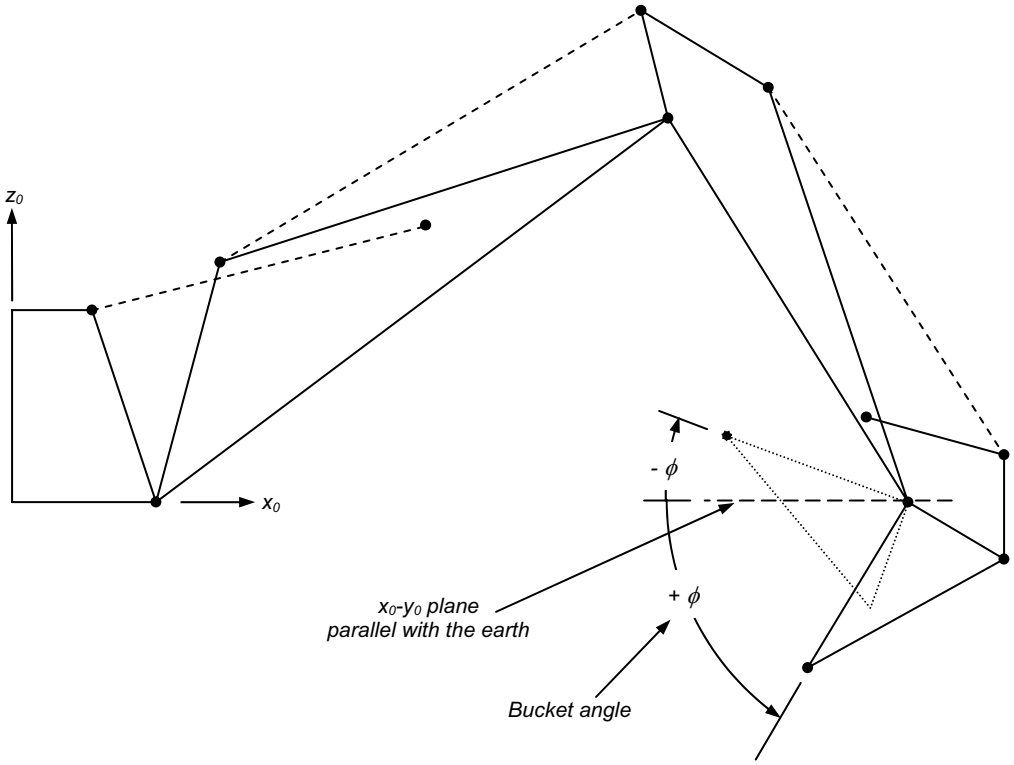

Cylinder Space to Joint Space Transformation

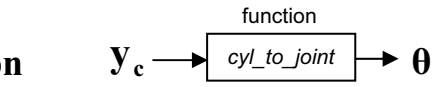

The following section derives the equations necessary to compute the joint angles from the cylinder lengths by analyzing each link independently from base to tip. All quantities are either known constants or functions of the input variables $y_c(i)$, and the equations represent the dynamic quantities that must be computed at each simulation step. All of the constant lengths and angles are either stored in memory or computed offline beforehand and have been omitted below for brevity. It is assumed that the cylinder lengths will be available from suitable linear position sensors mounted to the backhoe.

Figure 4: Link 1 Transformation

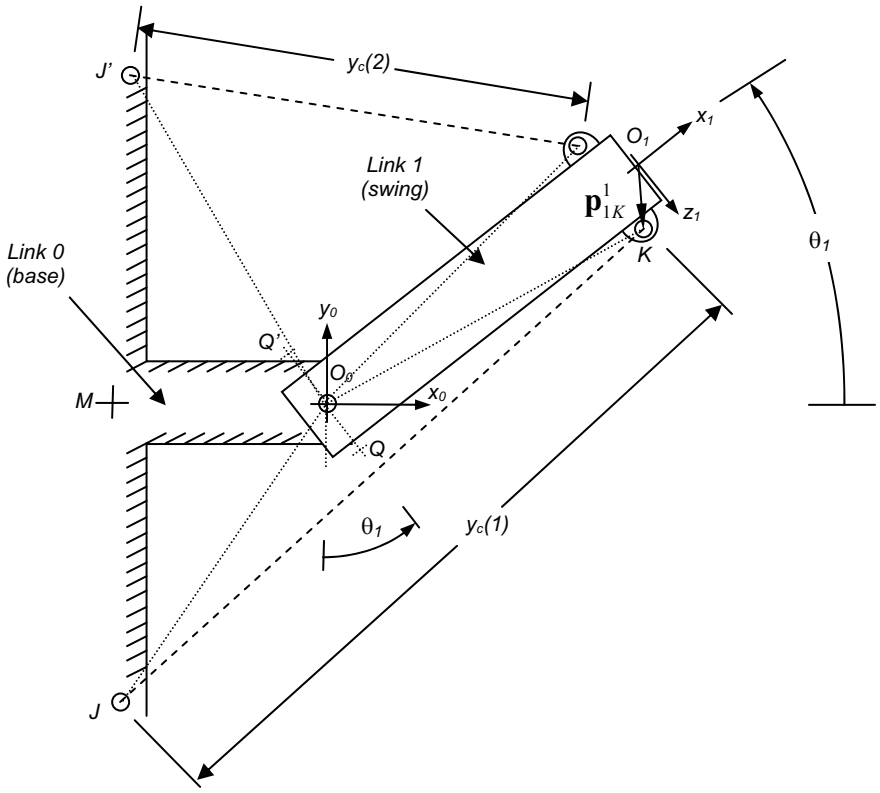

Figure 4 is a sketch of the base (tractor) and swing links as viewed from above.

The transformation from the known cylinder length $y_c(1)$ to the joint angle θ_1 is computed as follows.

$$\theta_{K0J} = \cos^{-1}\left(\frac{r_{0K}^2 + r_{0J}^2 - y_c^2(1)}{2r_{0K}r_{0J}}\right) \tag{1}$$

$$\theta_1 = \theta_{K0J} - \theta_{K0Q} - \theta_{MJ0} \tag{2}$$

Note that in practice, the angle θ_{K0J} must be checked to see whether it is greater than 180°, which requires knowledge of $y_c(2)$ as well.

Figure 5: Link 2 Transformation

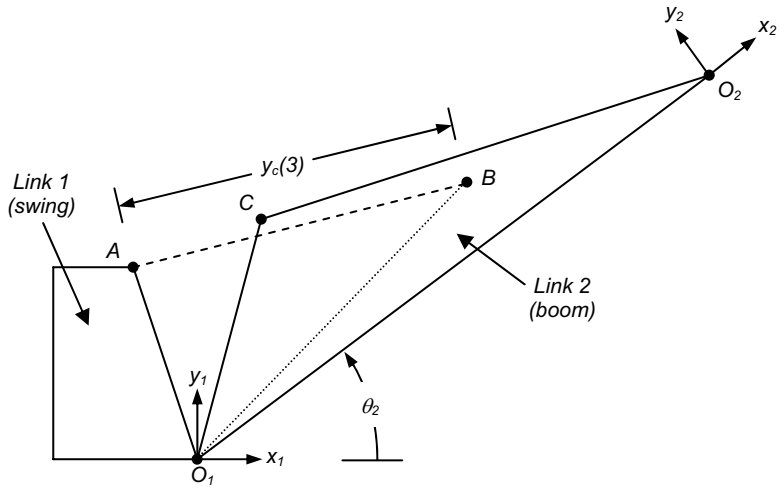

Figure 5 is a sketch of the swing and boom links as viewed from the side. The transformation from the boom cylinder length $y_c(3)$ to the joint angle θ_2 is as follows.

$$\theta_{A1B} = \cos^{-1}\left(\frac{r_{1A}^2 + r_{1B}^2 - y_c^2(3)}{2r_{1A}r_{1B}}\right) \tag{3}$$

$$\theta_2 = \pi - \theta_{01A} - \theta_{A1B} - \theta_{B12} \tag{4}$$

Figure 6: Link 3 Transformation

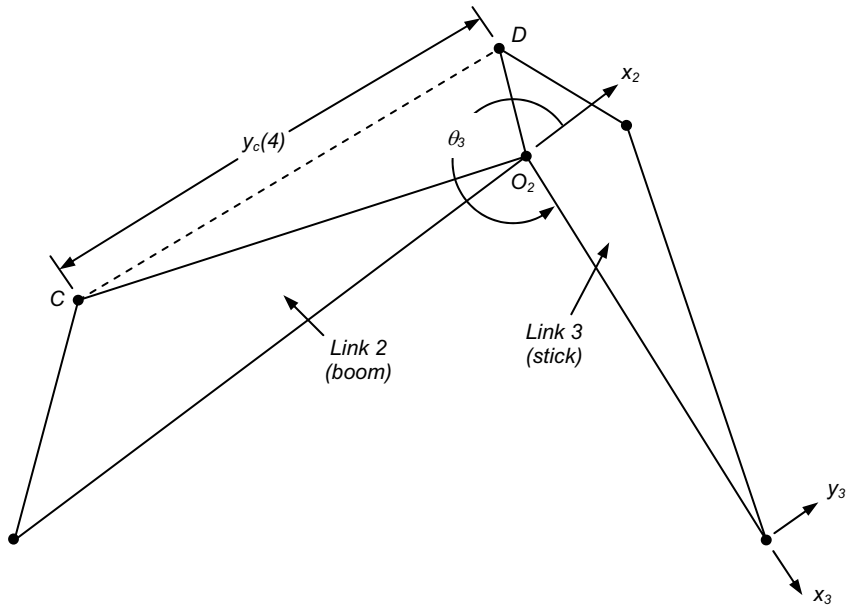

Figure 6 is a sketch of the boom and stick links as viewed from the side. The transformation from the stick cylinder length $y_c(4)$ to the joint angle θ_3 is as follows.

$$\theta_{C2D} = \cos^{-1}\left(\frac{r_{2C}^2 + r_{2D}^2 - y_c^2(4)}{2r_{2C}r_{2D}}\right) \tag{5}$$

$$\theta_3 = 3\pi - \theta_{12C} - \theta_{C2D} - \theta_{D23} \tag{6}$$

Figure 7 is a sketch of the stick and bucket links as viewed from the side. The transformation from the boom cylinder length $y_c(5)$ to the joint angle θ_4 is as follows.

Figure 7: Link 4 Transformation

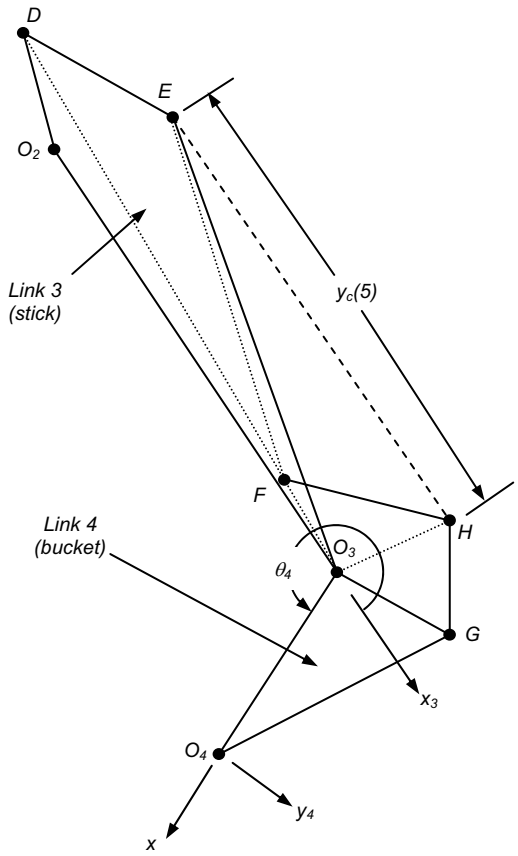

$$\theta_{EFH} = \cos^{-1}\left(\frac{r_{EF}^2 + r_{FH}^2 - y_c^2(5)}{2r_{EF}r_{FH}}\right) \tag{7}$$

$$\theta_{HF3} = \pi - \theta_{DFE} - \theta_{EFH} \tag{8}$$

$$r_{3H} = \sqrt{r_{3F}^2 + r_{FH}^2 - 2r_{3F}r_{FH}\cos(\theta_{HF3})} \tag{9}$$

$$\theta_{F3H} = \cos^{-1}\left(\frac{r_{3F}^2 + r_{3H}^2 - r_{FH}^2}{2r_{3F}r_{3H}}\right) \tag{10}$$

$$\theta_{H3G} = \cos^{-1}\left(\frac{r_{3H}^2 + r_{3G}^2 - r_{GH}^2}{2r_{3H}r_{3G}}\right) \tag{11}$$

$$\theta_4 = 3\pi - \theta_{F3H} - \theta_{H3G} - \theta_{G34} - \theta_{23D} \tag{12}$$

Thus with knowledge of the cylinder lengths $\mathbf{y_c}$, the joint angles $\boldsymbol{\theta}$ can be calculated from equations 1-12.

Forward Displacement Analysis

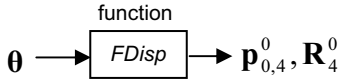

Using the Denavit-Hartenberg parameters listed in Table 1, the position and orientation of each component frame of the backhoe can be computed from the known joint angles θ_i, *i=1:4* by the successive multiplication of homogeneous transformations of the following form [1]:

$$\mathbf{A}_i^{i-1} = \left[\begin{array}{ccc:c} \cos(\theta_i) & -\sin(\theta_i)\cos(\alpha_i) & \sin(\theta_i)\sin(\alpha_i) & a_i\cos(\theta_i) \\ \sin(\theta_i) & \cos(\theta_i)\cos(\alpha_i) & -\cos(\theta_i)\sin(\alpha_i) & a_i\sin(\theta_i) \\ 0 & \sin(\alpha_i) & \cos(\alpha_i) & d_i \\ \hdashline 0 & 0 & 0 & 1 \end{array}\right] = \left[\begin{array}{cc} \mathbf{R}_i^{i-1} & \mathbf{p}_{i-1,i}^{i-1} \\ \mathbf{0}^{(1x3)} & 1 \end{array}\right] \quad (13)$$

where $\mathbf{R}_i^{i-1}$ is the 3x3 rotation matrix from frame *i-1* to frame *i* and $\mathbf{p}_{i-1,i}^{i-1}$ is the position vector of origin *i* with respect to origin *i-1* expressed in the *i-1* component frame.

The position and orientation of the end effector (ie bucket tip) is then computed from

$$\mathbf{B} = \mathbf{A}_1^0\mathbf{A}_2^1\mathbf{A}_3^2\mathbf{A}_4^3 = \left[\begin{array}{cc} \mathbf{R}_4^0 & \mathbf{p}_{0,4}^0 \\ \mathbf{0}^{(1x3)} & 1 \end{array}\right] \quad (14)$$

where **B** is termed the *bucket displacement matrix*. The rotation matrix $\mathbf{R}_4^0$ can be interpreted as a matrix of projections of the base frame unit vectors onto bucket frame unit vectors,

$$\mathbf{R}_4^0 = \left[\begin{array}{ccc} x_0\cdot x_4 & x_0\cdot y_4 & x_0\cdot z_4 \\ y_0\cdot x_4 & y_0\cdot y_4 & y_0\cdot z_4 \\ z_0\cdot x_4 & x_0\cdot y_4 & z_0\cdot z_4 \end{array}\right] \quad (15)$$

and $\mathbf{p}_{0,4}^0 = \left[p_{0,4}^0(x) \quad p_{0,4}^0(y) \quad p_{0,4}^0(z)\right]^T$ is the 3x1 position vector of the bucket tip relative to the base frame, expressed in base frame coordinates. Figure 8 illustrates the quantities computed by the bucket displacement matrix.

Figure 8: Bucket displacement matrix quantities

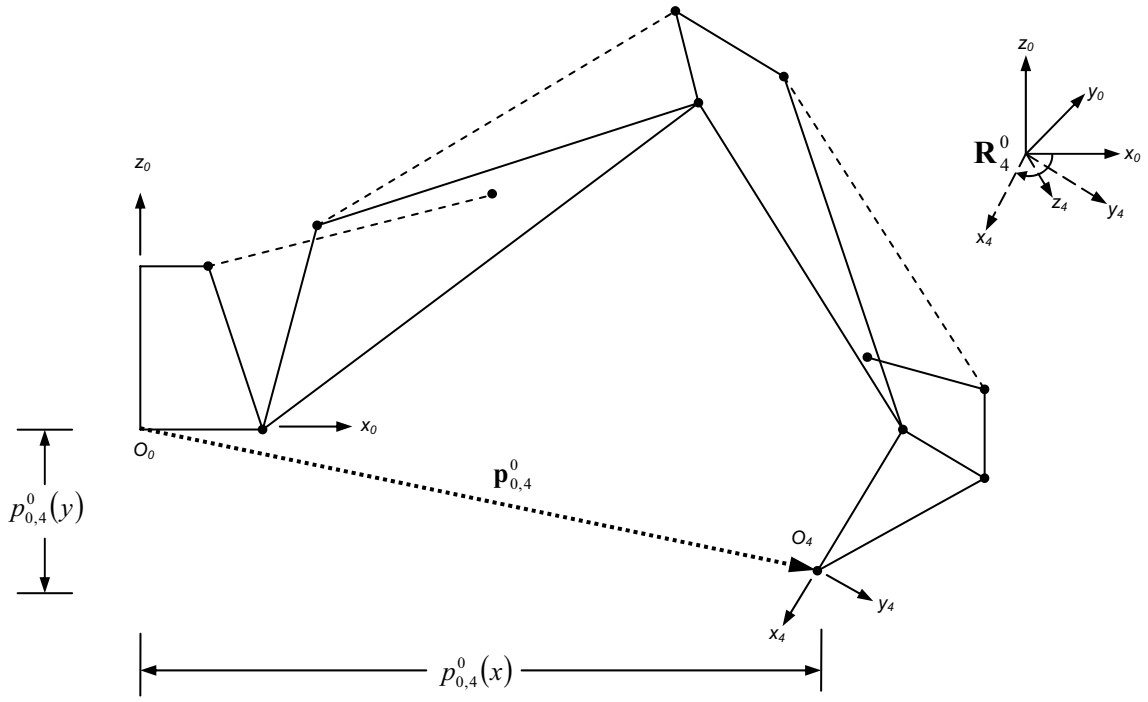

Once the bucket displacement matrix is computed, the bucket angle ϕ is then found from the x_4 vector relative to the x_0-y_0 plane. However, since the x_1 is constrained to rotate in the x_0-y_0 plane and y_1 is always parallel to z_0, the bucket angle is computed from

$$\phi = \text{atan2}\left(y_1 \cdot x_4, x_1 \cdot x_4\right) + \pi \tag{16}$$

Note that in Matlab, the output of the *atan2* function is limited to $-\pi < \phi < \pi$, so in the case that $x_1 \cdot x_4 < 0$ and $y_1 \cdot x_4 > 0$, the bucket is curled up tight next to the stick, and equation 16 becomes $\phi = \text{atan2}\left(\frac{z_0 \cdot x_4}{x_0 \cdot x_4}\right) - \pi$.

Thus the position and orientation of the bucket can be computed from knowledge of the joint angles by using equations 13, 14, and 16.

Reverse Displacement Analysis

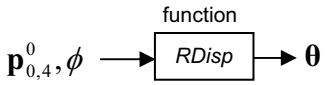

The reverse displacement analysis (RDA) is used to compute the vector of joint angles $\boldsymbol{\theta}$ from the bucket tip position $\mathbf{p}_{0,4}^{0}$ and the bucket angle ϕ. Figure 9 illustrates the quantities relevant to the RDA.

Figure 9: Reverse displacement vectors

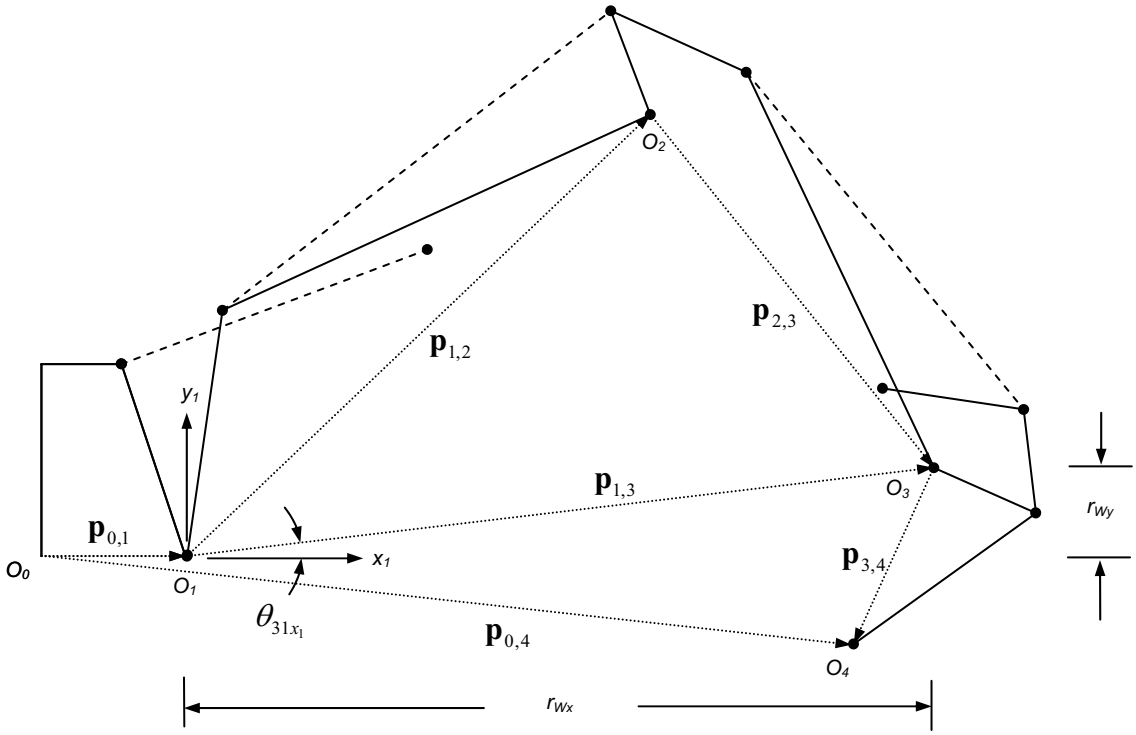

The swing angle θ_1 is decoupled from the other links and can be computed directly from the x and y components of the bucket position vector $\mathbf{p}_{0,4}^{0}$:

$$\theta_1 = \operatorname{atan2}\left(p_{0,4}^{0}(y), p_{0,4}^{0}(x)\right) \tag{17}$$

The remaining three links form a planar arm, and the joint angles are computed as follows. Using the rotation matrices R_1^0 and R_4^0 to express all vectors in frame 1,

$$\mathbf{p}_{1,3}^{1} = \mathbf{p}_{0,4}^{1} - \mathbf{p}_{0,1}^{1} - \mathbf{p}_{3,4}^{1} = \mathbf{R}_1^0 \mathbf{p}_{0,4}^{0} - \begin{bmatrix} a_1 \\ 0 \\ 0 \end{bmatrix} - \mathbf{R}_4^0 \begin{bmatrix} a_4 \\ 0 \\ 0 \end{bmatrix} \tag{18}$$

where $\mathbf{R}_4^0 = \mathbf{R}_1^0\mathbf{R}_2^1\mathbf{R}_3^2\mathbf{R}_4^3$. See Figure 9. The distance and angle formed from O_1 to the wrist O_3 is

$$r_{13} = \sqrt{\left(p_{1,3}^1(x)\right)^2 + \left(p_{1,3}^1(y)\right)^2} = \sqrt{\left(r_{Wx}\right)^2 + \left(r_{Wy}\right)^2} \tag{19}$$

$$\theta_{31x_1} = \tan^{-1}\left(\frac{p_{1,3}^1(y)}{p_{1,3}^1(x)}\right) = \tan^{-1}\left(\frac{r_{Wy}}{r_{Wx}}\right) \tag{20}$$

Now that all the sides of the triangle $O_1O_2O_3$ are known, the interior angles can be found using the cosine law,

$$\theta_{321} = \cos^{-1}\left(\frac{a_2^2 + a_3^2 - r_{13}^2}{2a_2a_3}\right) \tag{21}$$

$$\theta_{213} = \cos^{-1}\left(\frac{a_2^2 + r_{13}^2 - a_3^2}{2a_2r_{13}}\right) \tag{22}$$

and then the angles θ_2 and θ_3 can be found from

$$\theta_2 = \theta_{31x_1} + \theta_{213} \tag{23}$$

$$\theta_3 = \pi + \theta_{321} \tag{24}$$

Figure 10: θ_4 Geometry

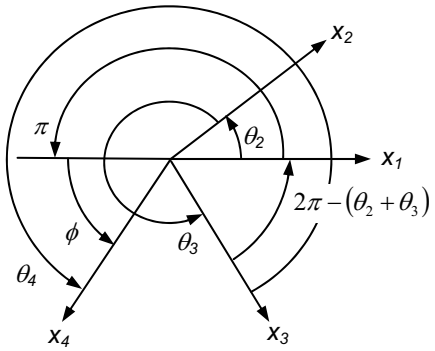

Figure 10 illustrates the relationship between the bucket angle ϕ and the joint angles θ_2, θ_3 and θ_4. The last angle θ_4 is then found from the bucket angle ϕ, where

$$\left[2\pi - \left(\theta_2 + \theta_3\right)\right] + \pi + \phi = \theta_4$$

or

$$\theta_4 = \phi - \theta_2 - \theta_3 + 3\pi \tag{25}$$

Joint Space to Cylinder Space Transformation

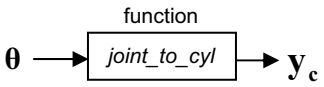

The joint space to cylinder space transformation is used to compute the cylinder lengths $\mathbf{y_c}$ from the joint angles $\boldsymbol{\theta}$. Combined with the reverse displacement algorithm, these routines are useful to compute the required cylinder length time histories for control purposes.

The lengths of the swing cylinders $y_c(1)$ and $y_c(2)$ are computed from θ_1 as follows.

$$\theta_{Q0J} = \tan^{-1}\left(\frac{r_{0M}}{r_{JM}}\right) + \theta_1 \tag{26}$$

$$\theta_{K0J} = \theta_{Q0J} + \frac{\pi}{2} - \theta_{10K} \tag{27}$$

$$y_c(1) = \sqrt{(r_{0J})^2 + (r_{0K})^2 - 2r_{0J}r_{0K}\cos(\theta_{K0J})} \tag{28}$$

$$\theta_{J'0Q'} = \tan^{-1}\left(\frac{r_{0M}}{r_{JM}}\right) - \theta_1 \tag{29}$$

$$\theta_{J'0K'} = \theta_{J'0Q'} + \frac{\pi}{2} - \theta_{10K} \tag{30}$$

$$y_c(2) = \sqrt{(r_{0J})^2 + (r_{0K})^2 - 2r_{0J}r_{0K}\cos(\theta_{J'0K'})} \tag{31}$$

Refer to Figure 4 for equations 26-31.

The boom cylinder length is found by rearranging equations 3 & 4:

$$\theta_{A1B} = \pi - \theta_{01A} - \theta_2 - \theta_{B12} \tag{32}$$

$$y_c(3) = \sqrt{(r_{1A})^2 + (r_{1B})^2 - 2r_{1A}r_{1B}\cos(\theta_{A1B})} \tag{33}$$

Refer to Figure 5 for equations 32 & 33.

The stick cylinder length is found by rearranging equations 5 & 6:

$$\theta_{C2D} = \pi - \theta_{D23} - \theta_{12C} - \theta_3 \tag{34}$$

$$y_c(4) = \sqrt{(r_{2C})^2 + (r_{2D})^2 - 2r_{2C}r_{2D}\cos(\theta_{C2D})} \tag{35}$$

The bucket cylinder length is found from four angle additions and four cosine laws. Refer to Figure 7 for equations 36-43.

$$\theta_{x_3 3G} = 2\pi - \theta_{G34} - \theta_4 \tag{36}$$

$$\theta_{G3F} = \pi - \theta_{x_3 3G} + \theta_{23D} \tag{37}$$

$$r_{FG} = \sqrt{(r_{3F})^2 + (r_{3G})^2 - 2r_{3F}r_{3G}\cos(\theta_{G3F})} \tag{38}$$

$$\theta_{3FG} = \cos^{-1}\left(\frac{r_{3F}^2 + r_{FG}^2 - r_{3G}^2}{2r_{3F}r_{FG}}\right) \tag{39}$$

$$\theta_{HFG} = \cos^{-1}\left(\frac{r_{FG}^2 + r_{FH}^2 - r_{GH}^2}{2r_{FG}r_{FH}}\right) \tag{40}$$

The angle θ_{HF3} depends on whether $\theta_4 + \theta_{G34} > 2\pi$:

$$\begin{aligned} &\text{if } \theta_4 + \theta_{G34} > 2\pi \\ &\quad \theta_{HF3} = \theta_{HFG} + \theta_{3FG} \\ &\text{otherwise} \\ &\quad \theta_{HF3} = \theta_{HFG} - \theta_{3FG} \end{aligned} \tag{41}$$

then

$$\theta_{EFH} = \pi - \theta_{DFE} + \theta_{HF3} \tag{42}$$

$$y_c(5) = \sqrt{(r_{EF})^2 + (r_{FH})^2 - 2r_{EF}r_{FH}\cos(\theta_{EFH})} \tag{43}$$

Actuator Force to Joint Torque Transformation

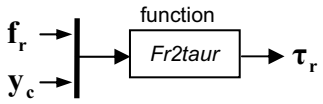

When simulating the backhoe's response to forces applied to the links by the hydraulic actuators, a transformation is necessary to convert from cylinder rod forces to joint torques. Formally, this step would involve replacing the rod forces $\mathbf{f_r}$ with a combination of both equivalent couple moments and forces. However, since we are only interested in the torque applied to the joints, the internal forces that intersect the joint axes will be neglected. Note that the magnitude of the applied joint torques $\boldsymbol{\tau}_\mathbf{r}$ depends on both the rod forces $\mathbf{f_r}$ and the cylinder lengths $\mathbf{y_c}$.

The first joint torque $\tau_r(1)$ at O_0 about the z_0 is computed from the contribution of the two swing cylinder forces $\mathbf{f_r}(1)$ and $\mathbf{f_r}(2)$. Figures 11 and 12 illustrate the transformation.

Figure 11: Swing cylinder transformation dimensions

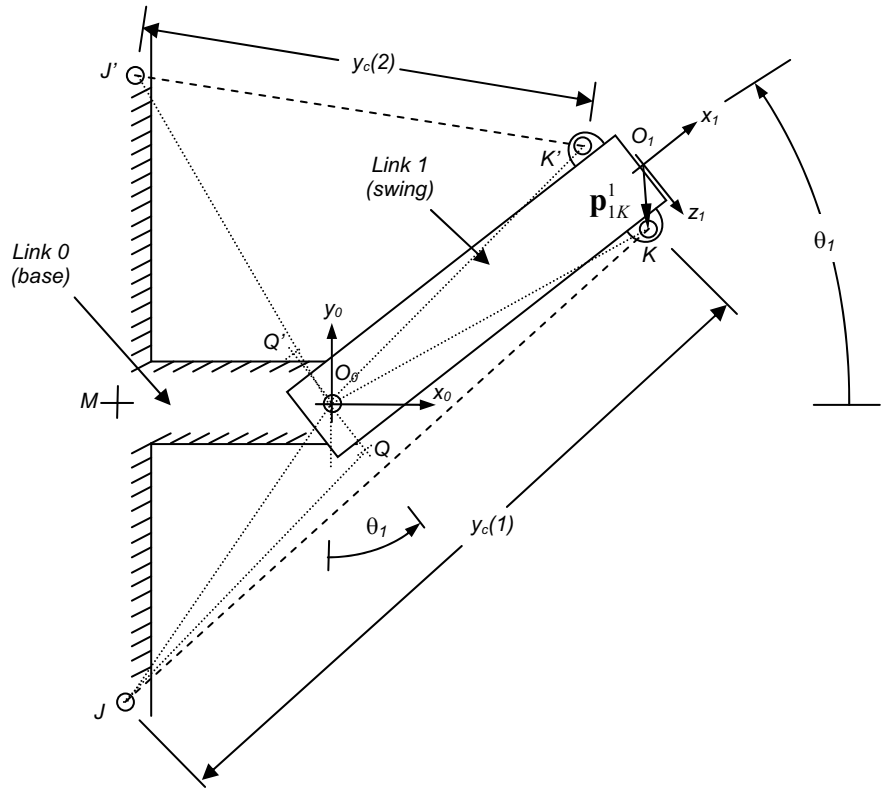

Figure 12: Swing cylinder force to joint 1 torque transformation

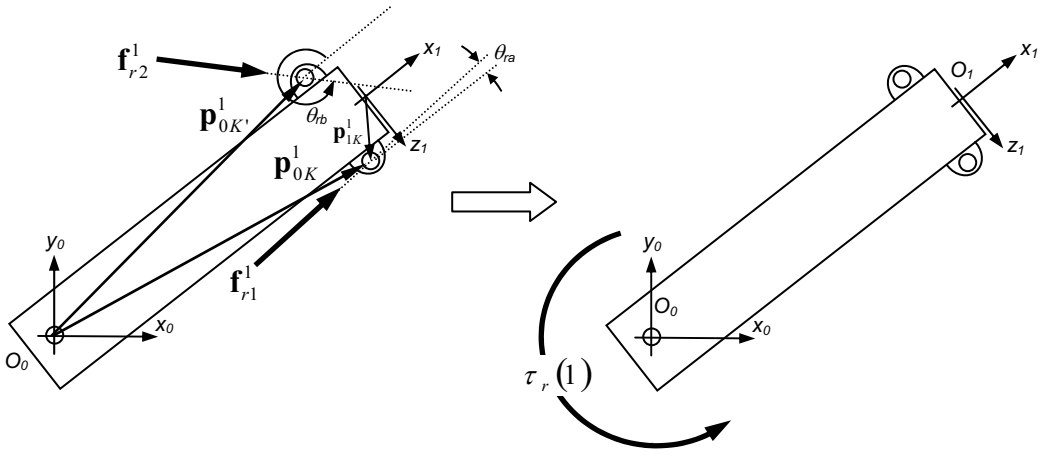

$$r_{JQ} = \sqrt{(r_{0J})^2 + (p^1_{1K}(3))^2 - 2r_{0J}p^1_{1K}(3)\cos(\theta_{Q0J})} \tag{44}$$

$$\theta_{r1} = \cos^{-1}\left(\frac{r^2_{QK} + y^2_c(1) - r^2_{JQ}}{2r_{QK}y_c(1)}\right) \tag{45}$$

$$r_{J'Q'} = \sqrt{(r_{0J'})^2 + (p^1_{1K}(3))^2 - 2r_{0J}p^1_{1K}(3)\cos(\theta_{J'0Q'})} \tag{46}$$

$$\theta_{r2} = 2\pi - \cos^{-1}\left(\frac{r^2_{QK} + y^2_c(2) - r^2_{J'Q'}}{2r_{QK}y_c(2)}\right) \tag{47}$$

$$\begin{aligned}\mathbf{p}^1_{0K} &= \begin{bmatrix} r_{QK} & 0 & p^1_{1K}(3)\end{bmatrix}^T \\ \mathbf{p}^1_{0K'} &= \begin{bmatrix} r_{QK} & 0 & -p^1_{1K}(3)\end{bmatrix}^T\end{aligned} \tag{48}$$

$$\begin{aligned}\mathbf{f}^1_{r1} &= |f_r(1)|\begin{bmatrix}\cos(\theta_{r1}) & 0 & \sin(\theta_{r1})\end{bmatrix}^T \\ \mathbf{f}^1_{r2} &= |f_r(2)|\begin{bmatrix}\cos(\theta_{r2}) & 0 & \sin(\theta_{r2})\end{bmatrix}^T\end{aligned} \tag{49}$$

$$\tau_r(1) = \left(\mathbf{p}^1_{0K} \times \mathbf{f}^1_{r1} + \mathbf{p}^1_{0K'} \times \mathbf{f}^1_{r2}\right) \cdot z_0 \tag{50}$$

Note that the five-element cylinder force vector $\mathbf{f_r}$ does not contain the direction information of the swing cylinder force vectors $\mathbf{f}^1_{r1}$ and $\mathbf{f}^1_{r2}$ used in equations 49-50; i.e.

$$\mathbf{f_r} = \begin{bmatrix} f_r(1) & f_r(2) & f_r(3) & f_r(4) & f_r(5)\end{bmatrix}^T \tag{51}$$

$$\mathbf{f_r} = \begin{bmatrix} f_r(swing_1) & f_r(swing_2) & f_r(boom) & f_r(stick) & f_r(bucket)\end{bmatrix}^T \tag{52}$$

which is related to equation 49 only by the magnitude of the first two elements.

Figures 13 and 14 illustrate the transformation of the force applied by the boom cylinder $\mathbf{f}_{r3}$ into the applied torque $\tau_r(2)$ at O_1 about z_1.

Figure 13: Boom cylinder transformation dimensions

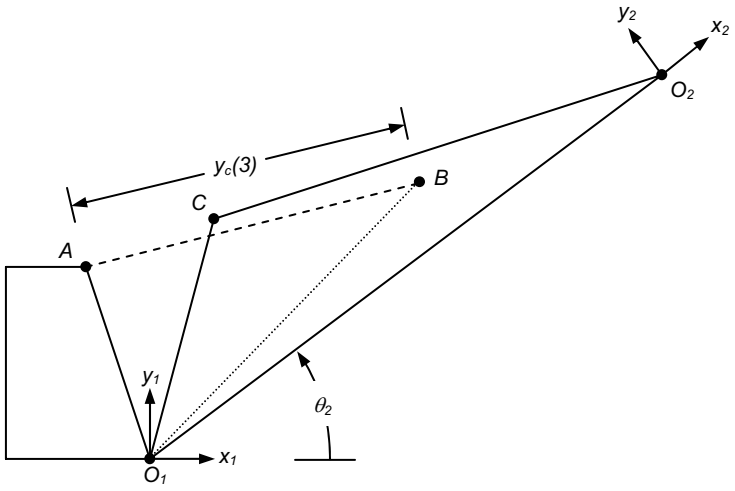

Figure 14: Boom cylinder force to joint 2 torque transformation

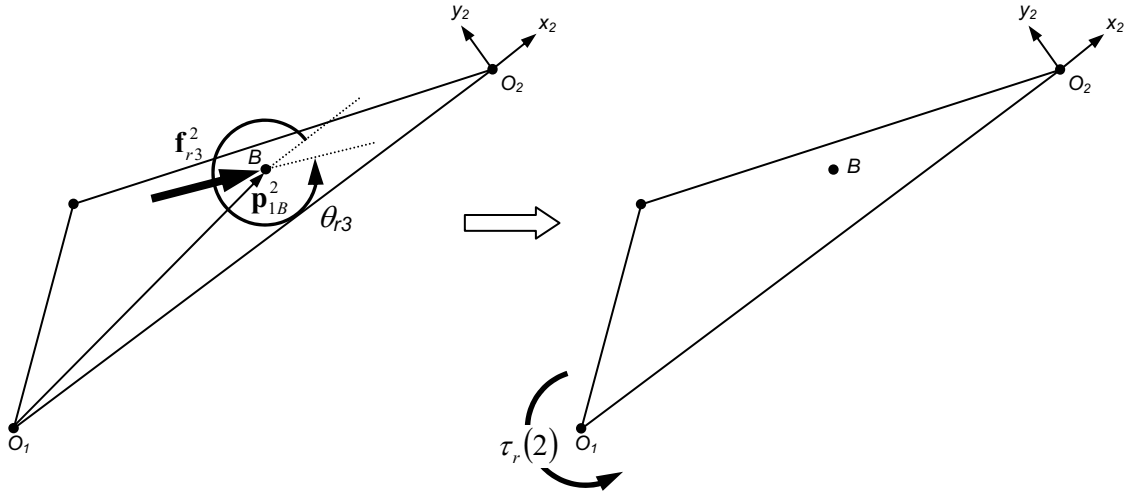

$$\theta_{1BA} = \cos^{-1}\left(\frac{y_c^2(3) + r_{1B}^2 - r_{1A}^2}{2y_c(3)r_{1B}}\right) \tag{53}$$

$$\theta_{r3} = 2\pi + \left(\theta_{B12} - \theta_{1BA}\right) \tag{54}$$

$$\mathbf{p}_{1B}^2 = r_{1B}\left[\cos(\theta_{B12}) \quad \sin(\theta_{B12}) \quad 0\right]^T \tag{55}$$

$$\mathbf{f}_{r3}^{2} = \left| f_r(3) \right| \left[\cos(\theta_{r3}) \quad \sin(\theta_{r3}) \quad 0 \right]^T \tag{56}$$

$$\tau_r(2) = \left(\mathbf{p}_{1B}^{2} \times \mathbf{f}_{r3}^{2} \right) \cdot z_1 \tag{57}$$

Figures 15 and 16 illustrate the transformation of the force applied by the stick cylinder $\mathbf{f}_{r4}$ into the applied torque $\tau_r(3)$ at O_2 about z_2.

Figure 15: Stick cylinder transformation dimensions

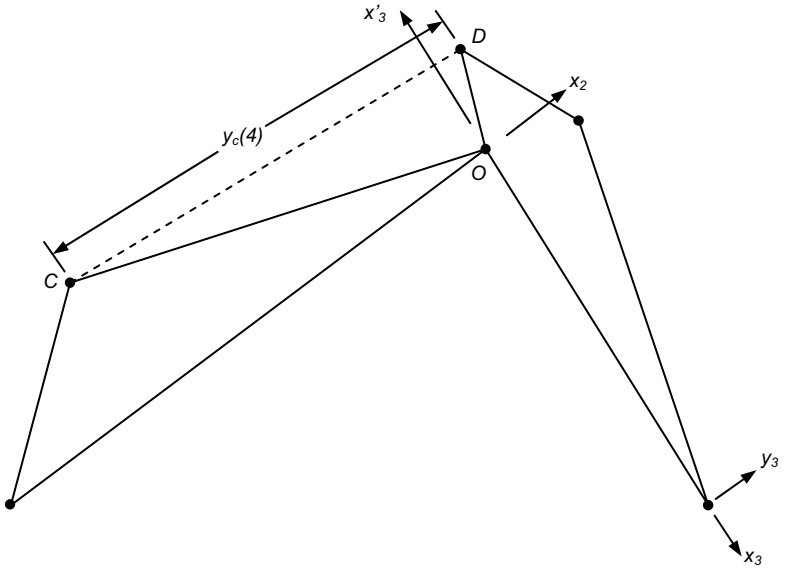

Figure 16: Stick cylinder force to joint 3 torque transformation

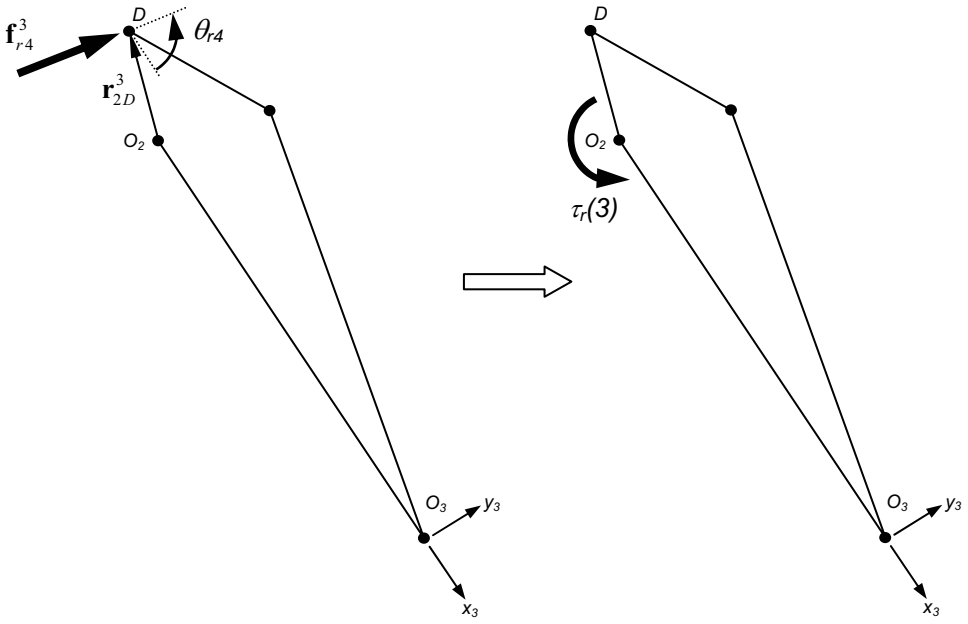

$$\theta_{2DC} = \cos^{-1}\left(\frac{r_{2D}^2 + y_c^2(4) - r_{2C}^2}{2r_{2D}y_c(4)}\right) \tag{58}$$

$$\theta_{x'_3 2D} = \pi - \theta_{D23} \tag{59}$$

$$\theta_{r4} = \pi - \theta_{2DC} - \theta_{x'_3 2D} \tag{60}$$

$$\mathbf{p}_{2D}^3 = r_{2D}\begin{bmatrix}\cos(\theta_{D23}) & \sin(\theta_{D23}) & 0\end{bmatrix}^T \tag{61}$$

$$\mathbf{f}_{r4}^3 = |f_r(4)|\begin{bmatrix}\cos(\theta_{r4}) & \sin(\theta_{r4}) & 0\end{bmatrix}^T \tag{62}$$

$$\tau_r(3) = \left(\mathbf{p}_{2D}^3 \times \mathbf{f}_{r4}^3\right)\cdot z_2 \tag{63}$$

Figure 17 illustrates the points of interest in computing the torque applied to the bucket. Knowledge of the force exerted by the bucket cylinder $\mathbf{f}_{r5}$ and the length of the bucket cylinder $y_c(5)$ is required for the transformation.

Figure 17: Bucket cylinder transformation dimensions

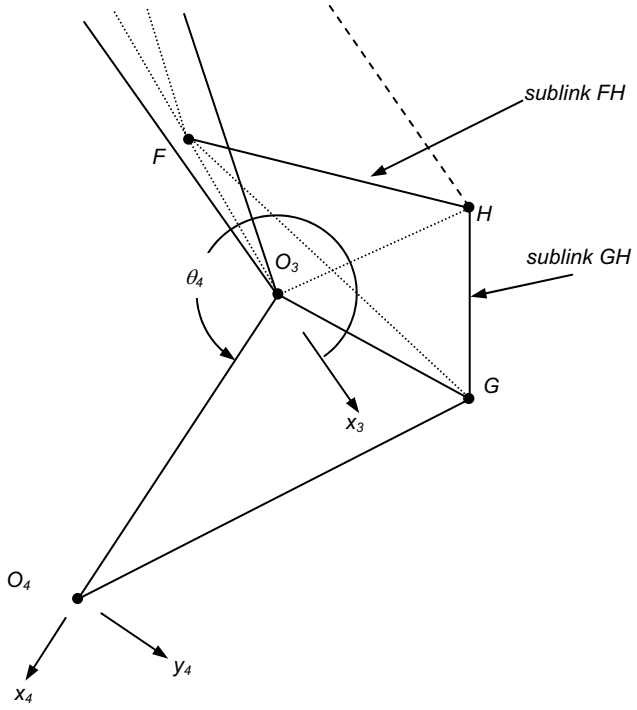

This transformation is solved by first analyzing the angles of the bucket sublinks *FH* and *GH* relative to the stick and bucket, summing forces at the pin connection at *H*, and finally solving simultaneously for the magnitude of the orthogonal components of the force $\mathbf{f}_G^4$ that link *GH* exerts on the bucket at point *G*.

Figures 18 illustrates the transformation of the force $\mathbf{f}_G^4$ exerted by the sublink *GH* onto the bucket, and the corresponding applied torque $\tau_r(4)$ at O_3 about z_3.

Figure 18: Bucket cylinder force to joint 4 torque transformation

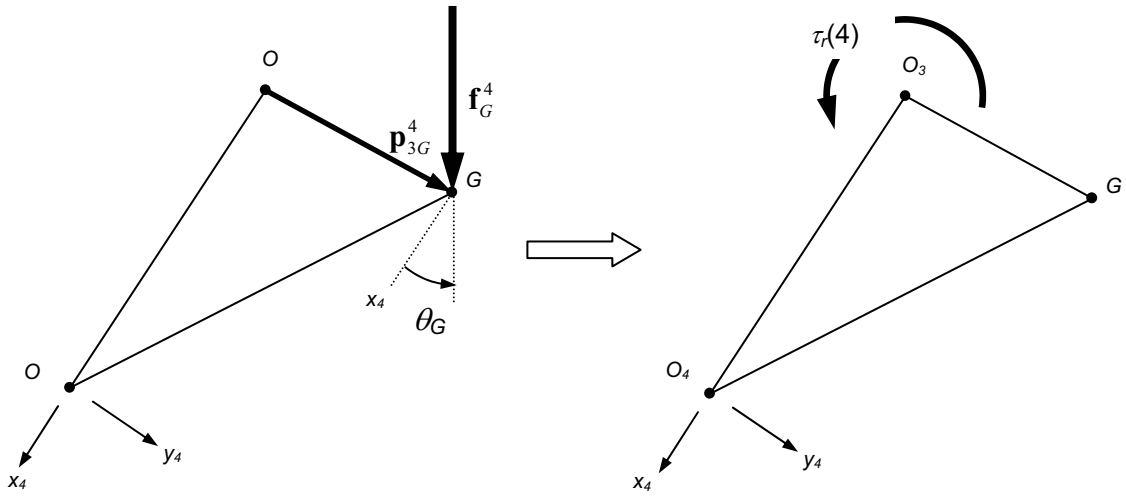

Figure 19(a) illustrates the geometry of the sublink *FH* relative to the stick. Figure 19(b) illustrates the forces applied to the pin at point *H*.

Figure 19: Sublink *FH* forces and geometry

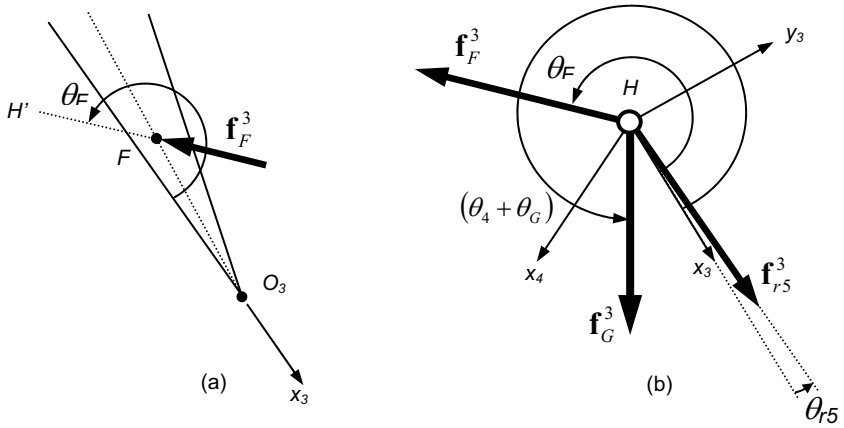

The first step is to find the angles θ_G, θ_{r5}, and θ_F:

$$\theta_{EFH} = \cos^{-1}\left(\frac{r_{EF}^2 + r_{FH}^2 - y_c^2(5)}{2r_{EF}r_{FH}}\right) \tag{64}$$

$$\theta_{HF3} = \pi - \theta_{DFE} - \theta_{EFH} \tag{65}$$

$$r_{3H} = \sqrt{r_{3F}^2 + r_{FH}^2 - 2r_{3F}r_{FH}\cos(\theta_{HF3})} \tag{66}$$

$$\theta_{F3H} = \cos^{-1}\left(\frac{r_{3F}^2 + r_{3H}^2 - r_{FH}^2}{2r_{3F}r_{3H}}\right) \tag{67}$$

$$\theta_{H3G} = \cos^{-1}\left(\frac{r_{3H}^2 + r_{3G}^2 - r_{GH}^2}{2r_{3H}r_{3G}}\right) \tag{68}$$

$$\theta_4 = 3\pi - \theta_{F3H} - \theta_{H3G} - \theta_{G34} - \theta_{23D} \tag{69}$$

$$\theta_{x_3 3G} = 2\pi - \theta_4 - \theta_{G34} \tag{70}$$

The angle θ_{G3F} depends on whether $\theta_4 + \theta_{G34} > 2\pi$:

$$\begin{aligned} &\text{if } \theta_4 + \theta_{G34} > 2\pi \\ &\quad \theta_{G3F} = \pi - \theta_{x_3 3G} - \theta_{23D} \\ &\text{otherwise} \\ &\quad \theta_{G3F} = \pi - \theta_{x_3 3G} + \theta_{23D} \end{aligned} \tag{71}$$

$$r_{FG} = \sqrt{(r_{3F})^2 + (r_{3G})^2 - 2r_{3F}r_{3G}\cos(\theta_{G3F})} \tag{72}$$

$$\theta_{FG3} = \cos^{-1}\left(\frac{r_{FG}^2 + r_{3G}^2 - r_{3F}^2}{2r_{FG}r_{3G}}\right) \tag{73}$$

$$\theta_{FGH} = \cos^{-1}\left(\frac{r_{FG}^2 + r_{GH}^2 - r_{FH}^2}{2r_{FG}r_{GH}}\right) \tag{74}$$

The angle θ_{3GH} depends on whether $\theta_4 + \theta_{G34} > 2\pi$:

$$\begin{aligned} &\text{if } \theta_4 + \theta_{G34} > 2\pi \\ &\quad \theta_{3GH} = \theta_{FGH} - \theta_{FG3} \\ &\text{otherwise} \\ &\quad \theta_{3GH} = \theta_{FGH} + \theta_{FG3} \end{aligned} \tag{75}$$

The angle θ_G is defined as the angle that the two-force link GH makes with x_4:

$$\theta_G = \theta_{G34} - \theta_{3GH} \tag{76}$$

$$\theta_{3FG} = \cos^{-1}\left(\frac{r_{3F}^2 + r_{FG}^2 - r_{3G}^2}{2r_{3F}r_{FG}}\right) \tag{77}$$

$$\theta_{HFG} = \cos^{-1}\left(\frac{r_{FG}^2 + r_{FH}^2 - r_{GH}^2}{2r_{FG}r_{FH}}\right) \tag{78}$$

The angle θ_{HF3} depends on whether $\theta_4 + \theta_{G34} > 2\pi$:

$$\begin{aligned} &\text{if } \theta_4 + \theta_{G34} > 2\pi \\ &\quad \theta_{HF3} = \theta_{HFG} + \theta_{3FG} \\ &\text{otherwise} \\ &\quad \theta_{HF3} = \theta_{HFG} - \theta_{3FG} \end{aligned} \tag{79}$$

$$\theta_{3FH'} = \pi - \theta_{HF3} \tag{80}$$

$$\theta_F = \left(\pi - \theta_{3FH'} - \theta_{23D}\right) + \pi \tag{81}$$

$$\theta_{FHE} = \cos^{-1}\left(\frac{r_{FH}^2 + y_c^2(5) - r_{EF}^2}{2r_{FH}\,y_c(5)}\right) \tag{82}$$

$$\theta_{r5} = -\theta_{23D} + \theta_{HF3} - \theta_{FHE} \tag{83}$$

Now that the angles θ_G, θ_F, and θ_{r5} are known from equations 76, 81, and 83, a force balance on pin H in the x_3 and y_3 directions yields

$$\begin{aligned} f_{r5}\cos(\theta_{r5}) + f_F\cos(\theta_F) + f_G\cos(\theta_4 + \theta_G) &= 0 \\ f_{r5}\sin(\theta_{r5}) + f_F\sin(\theta_F) + f_G\sin(\theta_4 + \theta_G) &= 0 \end{aligned} \tag{84}$$

where the mass of pin H has been neglected. Rearranging (84) into matrix format and solving for the magnitudes of the unknown forces $\mathbf{f}_F$ and $\mathbf{f}_G$,

$$\begin{bmatrix} f_F \\ f_G \end{bmatrix} = \begin{bmatrix} \cos(\theta_F) & \cos(\theta_4 + \theta_G) \\ \sin(\theta_F) & \sin(\theta_4 + \theta_G) \end{bmatrix}^{-1} \begin{bmatrix} -f_{r5}\cos(\theta_{r5}) \\ -f_{r5}\sin(\theta_{r5}) \end{bmatrix} \tag{85}$$

See Figure 19(b).

The torque $\tau_r(4)$ applied to the bucket at O_3 about z_3 by the force f_G is then found from

$$\mathbf{p}_{3G}^4 = r_{3G}\begin{bmatrix}\cos(\theta_{G34}) & \sin(\theta_{G34}) & 0\end{bmatrix}^T \tag{86}$$

$$\mathbf{f}_G^4 = f_G\begin{bmatrix}\cos(\theta_G) & \sin(\theta_G) & 0\end{bmatrix}^T \tag{87}$$

$$\tau_r(4) = \left(\mathbf{p}_{3G}^4 \times \mathbf{f}_G^4\right)\cdot z_3 \tag{89}$$

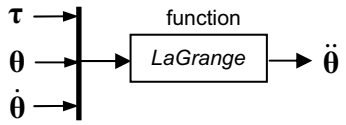

In the field of robotics, a common approach to the dynamic modeling of serial manipulators is to use the principles laid out by Joseph-Louis LaGrange in 1788 in his work entitled the *Mécanique analytique* [1], [2], [3]. Unlike the Newton-Euler approach, the LaGrangian approach bases its equations of motion on the kinetic and potential energy of the system in terms of a set of generalized coordinates, which are the rotational and translational positions and velocities of the robot's joints. The advantage to the LaGrangian approach is that there is no need to compute reaction forces at the connections between links, which are typically of no interest to the analysis.

The LaGrangian function is defined as the difference between the kinetic and potential energy of the mechanical system:

$$L = K - U \tag{90}$$

where K is the scalar sum of the kinetic energy of all the links

$$K = \frac{1}{2}\sum_{i=1}^{n} \mathbf{v}_{ci}^{T}\mathbf{m}_{i}\mathbf{v}_{ci} + \boldsymbol{\omega}_{i}^{T}\mathbf{I}_{i}\boldsymbol{\omega}_{i} \tag{91}$$

and U is the scalar sum of the potential energy of all the links

$$U = -\sum_{i=1}^{n} m_{i}\mathbf{g}^{T}\mathbf{p}_{0,c_i} \tag{92}$$

In equation 91, $\mathbf{v}_{ci}$ is the 3x1 translational velocity vector of link i written at the center of mass, and $\boldsymbol{\omega}_i$ is the 3x1 rotational velocity vector of link i, both relative to the base frame. The mass matrix $\mathbf{m}_i$ is the diagonal 3x3 matrix where $\mathbf{m}_i$=diag([m_i m_i m_i]), and the lower case has been used to reserve the upper case **M** for the results of the present formulation. The inertia matrix $\mathbf{I}_i$ is the diagonal 3x3 inertia tensor containing the three principle inertias.

In equation 92, the negative sign accounts for the fact that the gravitational vector $\mathbf{g}$=[0 0 $-g$]^{T} points in the negative z_0 direction. Also, both the gravitational vector **g** and the position vector of the center of mass relative to the base frame $\mathbf{p}_{0,c_i}$ are expressed in base frame coordinates and the superscripts have been omitted for brevity. The index n is the number of degrees of freedom of the system.

Equation 91 can be rewritten by using the theory of instantaneous screw motion [4] by defining the relationship between the velocities of each link $\mathbf{v}_{ci}$ and $\boldsymbol{\omega}_i$ and the joint rates $\dot{\boldsymbol{\theta}}$ using the geometric *Jacobian* matrix:

$$\mathbf{J}_{vi} = \begin{bmatrix} \mathbf{J}_{vi}^{1} & \mathbf{J}_{vi}^{2} \ldots & \mathbf{J}_{vi}^{i} & \mathbf{0} & \mathbf{0} \ldots & \mathbf{0} \end{bmatrix} \tag{93}$$

$$\mathbf{J}_{\omega i} = \begin{bmatrix} \mathbf{J}_{\omega i}^{1} & \mathbf{J}_{\omega i}^{2} \ldots & \mathbf{J}_{\omega i}^{i} & \mathbf{0} & \mathbf{0} \ldots & \mathbf{0} \end{bmatrix} \tag{94}$$

where the elements of the *3×n link Jacobian submatrices* $\mathbf{J}_{vi}$ and $\mathbf{J}_{wi}$ are defined by

$$\mathbf{J}_{vi}^{j} = \begin{cases} z_{j-1} \times \mathbf{p}_{j-1,ci}^{j-1} & \text{for a revolute joint} \\ z_{j-1} & \text{for a prismatic joint} \end{cases} \tag{95}$$

$$\mathbf{J}_{\omega i}^{j} = \begin{cases} z_{j-1} & \text{for a revolute joint} \\ \mathbf{0}^{(3x1)} & \text{for a prismatic joint} \end{cases} \tag{96}$$

and *j=1:i*. The vector $\mathbf{p}_{j-1,ci}^{j-1}$ is the position of the current link's center of mass relative to the previous link's origin expressed in the previous link's coordinates. Note that the complete Jacobian matrix

$$\mathbf{J}_i = \begin{bmatrix} \mathbf{J}_{vi} \\ \mathbf{J}_{\omega i} \end{bmatrix} \tag{97}$$

is written separately for each link.

With the Jacobian matrices defined for each link, the linear and angular velocities of each link can be written in the generalized coordinates as

$$\begin{bmatrix} \mathbf{v}_{ci} \\ \boldsymbol{\omega}_i \end{bmatrix} = \begin{bmatrix} \mathbf{J}_{vi} \\ \mathbf{J}_{\omega i} \end{bmatrix} \dot{\boldsymbol{\theta}} \tag{98}$$

Substituting the components of equation 98 into 91 yields

$$K = \frac{1}{2} \dot{\boldsymbol{\theta}}^T \left(\sum_{i=1}^{n} \mathbf{J}_{vi}^T \mathbf{m}_i \mathbf{J}_{vi} + \mathbf{J}_{\omega i}^T \mathbf{I}_i \mathbf{J}_{\omega i} \right) \dot{\boldsymbol{\theta}} \tag{99}$$

The quantity in parenthesis in equation 99 is termed the *n×n manipulator inertia matrix* $\mathbf{M}$, where

$$\mathbf{M} = \sum_{i=1}^{n} \left(\mathbf{J}_{vi}^T \mathbf{m}_i \mathbf{J}_{vi} + \mathbf{J}_{\omega i}^T \mathbf{I}_i \mathbf{J}_{\omega i} \right) \tag{100}$$

so that

$$K = \frac{1}{2}\dot{\boldsymbol{\theta}}^T \mathbf{M} \dot{\boldsymbol{\theta}} \tag{101}$$

Now we are ready to form the equations of motions in terms of the generalized coordinates. Substituting 92 and 101 into 90 yields

$$L = \frac{1}{2}\dot{\boldsymbol{\theta}}^T \mathbf{M} \dot{\boldsymbol{\theta}} + \sum_{i=1}^{n} m_i \mathbf{g}^T \mathbf{p}_{0,c_i} \tag{102}$$

The equations of motion can now be described by taking the derivative of equation 102 with respect to $\boldsymbol{\theta}$, $\dot{\boldsymbol{\theta}}$, and time *t*:

$$\frac{d}{dt}\left(\frac{\partial L}{\partial \dot{\theta}_i}\right) - \frac{\partial L}{\partial \theta_i} = \tau_i \tag{103}$$

Substituting equation 90 into 103, this becomes

$$\frac{d}{dt}\left(\frac{\partial K}{\partial \dot{\theta}_i}\right) - \frac{\partial K}{\partial \theta_i} - \frac{\partial U}{\partial \theta_i} = \tau_i \tag{104}$$

where we have used the fact the *K* is a function of both $\boldsymbol{\theta}$ and $\dot{\boldsymbol{\theta}}$, but *U* is only a function of $\boldsymbol{\theta}$. The joint torque τ_i is the torque of link *i-1* acting on link *i* along the z_{i-1} axis. Note that τ_i may be a sum of torques from more than one source, such as from both actuator forces and forces applied to the end effector.

Evaluating the first term in equation 104 yields

$$\frac{d}{dt}\left(\frac{\partial K}{\partial \dot{\theta}_i}\right) = \sum_{j=1}^{n} M_{ij}\ddot{\theta}_j + \sum_{j=1}^{n}\sum_{k=1}^{n} \frac{\partial M_{ij}}{\partial \theta_k}\dot{\theta}_j \dot{\theta}_k \tag{105}$$

where the manipulator inertia matrix has been expanded into a sum of scalar elements before the product rule has been applied.

Evaluating the second term of equation 104 yields

$$\frac{\partial K}{\partial \theta_i} = \frac{1}{2}\sum_{j=1}^{n}\sum_{k=1}^{n} \frac{\partial M_{jk}}{\partial \theta_i}\dot{\theta}_j \dot{\theta}_k \tag{106}$$

and evaluating the third term of equation 104 yields

$$\frac{\partial U}{\partial \theta_i} = -\sum_{j=1}^{n} m_j \mathbf{g}^T \mathbf{J}_{vj}^{i} \tag{107}$$

where the fact that $\frac{\partial \mathbf{p}_{0,cj}}{\partial \theta_i} = \frac{\partial \mathbf{p}_{j-1,cj}}{\partial \theta_i} = \mathbf{J}_{vj}^{i}$ has been used from equation 95. Substituting equations 105-107 into 104 and combining terms yields the final form of the LaGrangian dynamic equation:

$$\sum_{j=1}^{n} M_{ij}\ddot{\theta}_j + \sum_{j=1}^{n}\sum_{k=1}^{n}\left(\frac{\partial M_{ij}}{\partial \theta_k} - \frac{1}{2}\frac{\partial M_{jk}}{\partial \theta_i}\right)\dot{\theta}_j\dot{\theta}_k - \sum_{j=1}^{n} m_j \mathbf{g}^T \mathbf{J}_{vj}^{i} = \tau_i \qquad (108)$$

which is valid for each degree of freedom, *i=1:n*. Each of the n equations of the form given by 61 can be written more compactly in matrix form:

$$\mathbf{M}(\boldsymbol{\theta})\ddot{\boldsymbol{\theta}} + \mathbf{V}(\boldsymbol{\theta},\dot{\boldsymbol{\theta}}) + \mathbf{G}(\boldsymbol{\theta}) = \boldsymbol{\tau} \qquad (109)$$

where

$$\mathbf{V} = \sum_{j=1}^{n}\sum_{k=1}^{n}\left(\frac{\partial M_{ij}}{\partial \theta_k} - \frac{1}{2}\frac{\partial M_{jk}}{\partial \theta_i}\right)\dot{\theta}_j\dot{\theta}_k \qquad (110)$$

$$\mathbf{G} = -\sum_{j=1}^{n} m_j \mathbf{g}^T \mathbf{J}_{vj}^{i} \qquad (111)$$

and **M** is given in equation 100. The vector **V** is called the velocity coupling vector, which contains the velocity-dependent centripetal and coriolis terms, and the vector **G** is called the vector of gravitational torques. The variables **V** and **G** have been left as capitals to be consistent with the literature. Figure 20 is a block diagram of the relevant portion of the backhoe simulation.

Figure 20: LaGrangian dynamics simulation block diagram

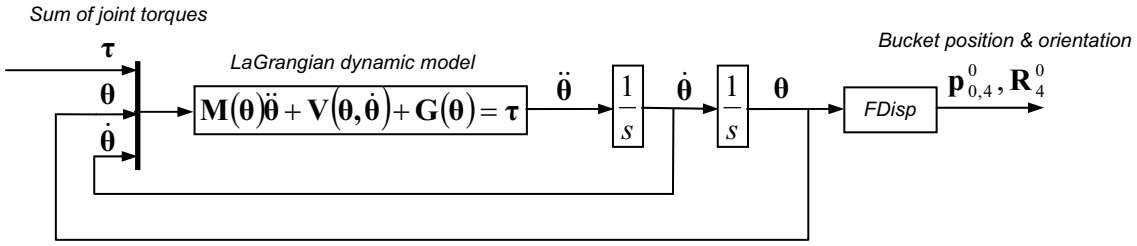

Thus the bucket position and orientation can be computed from the applied joint torques, along with the necessary initial joint positions $\boldsymbol{\theta}$ and velocities $\dot{\boldsymbol{\theta}}$ at *t=0*.

The dynamic model given by equation 109 was constructed using CAD software for the mass and inertia properties, and simulation software to compute the dynamic quantities. The elements of the variables **M**, **V**, and **G** given by equations 100, 110, and 111 were manipulated with software and the results are listed in the Appendix along with the mass and inertia properties calculated from the solid modeling software.

References

[1] Sciavicco, L., Siciliano, B., *Modeling and Control of Robot Manipulators, 2nd ed.* Springer-Verlag, London, 2001

[2] Tsai, L.W. *Robot Analysis*. John Wiley & Sons, NY, 1999.

[3] Craig, J.J., *Introduction to Robotics*. Addison-Wesley Pub. Co., Reading, MA, 1989.

[4] Lipkin, H., Duffy, J., "Sir Robert Stawell Ball and methodologies of modern screw theory". *J Mechanical Engineering Science, Proc Instn Mech Engrs Vol 216 Part C*, 2002.

Appendix

Mass and Inertia Properties from ProENGINEER

BASE ASSEMBLY WITH CYLINDERS

VOLUME = 3.2541377e+02 INCH^3
SURFACE AREA = 1.5227593e+03 INCH^2
AVERAGE DENSITY = 2.2985860e-01 POUND / INCH^3
MASS = 7.4799154e+01 POUND

CENTER OF GRAVITY with respect to ASM_DEF_CSYS coordinate frame:
X Y Z -7.9450335e+00 3.2953767e+00 6.6521587e-02 INCH

INERTIA at CENTER OF GRAVITY with respect to ASM_DEF_CSYS coordinate frame:
(POUND * INCH^2)

INERTIA TENSOR:
Ixx Ixy Ixz 2.3229143e+03 -5.2539074e+02 5.7118446e+01
Iyx Iyy Iyz -5.2539074e+02 5.2772512e+03 1.0302013e+01
Izx Izy Izz 5.7118446e+01 1.0302013e+01 5.3568896e+03

BOOM ASSEMBLY WITH CYLINDER

VOLUME = 4.9585884e+02 INCH^3
SURFACE AREA = 3.4438223e+03 INCH^2
AVERAGE DENSITY = 2.1966004e-01 POUND / INCH^3
MASS = 1.0892037e+02 POUND

CENTER OF GRAVITY with respect to ASM_DEF_CSYS coordinate frame:
X Y Z -2.6439663e+01 3.1270699e+00 0.0000000e+00 INCH

INERTIA at CENTER OF GRAVITY with respect to ASM_DEF_CSYS coordinate frame:
(POUND * INCH^2)

INERTIA TENSOR:
Ixx Ixy Ixz 2.0186501e+03 7.6399946e+02 0.0000000e+00
Iyx Iyy Iyz 7.6399946e+02 1.5264085e+04 0.0000000e+00
Izx Izy Izz 0.0000000e+00 0.0000000e+00 1.6083935e+04

STICK ASSEMBLY WITH CYLINDER

VOLUME = 4.5121342e+02 INCH^3
SURFACE AREA = 3.1935502e+03 INCH^2
AVERAGE DENSITY = 2.1115129e-01 POUND / INCH^3
MASS = 9.5274297e+01 POUND

CENTER OF GRAVITY with respect to ASM_DEF_CSYS coordinate frame:
X Y Z -2.3363210e+01 2.8479407e+00 0.0000000e+00 INCH

INERTIA at CENTER OF GRAVITY with respect to ASM_DEF_CSYS coordinate frame:
(POUND * INCH^2)

INERTIA TENSOR:
Ixx Ixy Ixz 1.3518286e+03 -5.4510614e+02 0.0000000e+00
Iyx Iyy Iyz -5.4510614e+02 2.2033641e+04 0.0000000e+00
Izx Izy Izz 0.0000000e+00 0.0000000e+00 2.2529499e+04

```
BUCKET ASSEMBLY WITH CYLINDER
-----------------------------

VOLUME =  2.2684190e+02  INCH^3
SURFACE AREA =  1.7929021e+03  INCH^2
AVERAGE DENSITY =  2.8400000e-01 POUND / INCH^3
MASS =  6.4423099e+01 POUND

CENTER OF GRAVITY with respect to ASM_DEF_CSYS coordinate frame:
X   Y   Z     7.7946254e+00  3.3482795e+00 -7.3503549e-04  INCH

INERTIA at CENTER OF GRAVITY with respect to ASM_DEF_CSYS coordinate frame:
(POUND * INCH^2)

INERTIA TENSOR:
Ixx Ixy Ixz  2.0413482e+03 -4.5279092e+02  5.9602768e-01
Iyx Iyy Iyz -4.5279092e+02  6.2054163e+03 -9.1988628e-02
Izx Izy Izz  5.9602768e-01 -9.1988628e-02  5.9272355e+03
```

Dynamic Model Elements from Matlab

The code that follows is the results of symbolic manipulations from equations 100, 110, and 111, generated using Matlab's symbolic math toolbox. Note that the joint angles are given in terms of the variable q rather than θ. The LaGrangian dynamic model is given by

$$\mathbf{M}(\mathbf{q})\ddot{\mathbf{q}} + \mathbf{V}(\mathbf{q},\dot{\mathbf{q}}) + \mathbf{G}(\mathbf{q}) = \boldsymbol{\tau}$$

where the elements of the matrix **M** *and the vectors* **V** *and* **G** *are given below.*

M(1,1) = 1/2*m2*p2x^2+m3*p3z^2+m3*a1^2+m2*p2z^2+m2*a1^2+m1*p1z^2-
1/2*I311*cos(2*q(3)+2*q(2))+1/2*m2*p2x^2*cos(2*q(2))-
1/2*m2*p2y^2*cos(2*q(2))+I122+1/2*m2*p2y^2+2*m2*cos(q(2))*p2x*a1-
2*m2*sin(q(2))*p2y*a1+m4*p4z^2+1/2*m4*a2^2+2*m3*cos(q(2))*a2*a1+1/2*m3*p3
x^2+1/2*I422*cos(2*q(4)+2*q(3)+2*q(2))+m3*p3x*a2*cos(q(3))-
m3*p3y*a2*sin(q(3))-1/2*m3*p3y^2*cos(2*q(3)+2*q(2))-
2*m3*p3y*a1*sin(q(3)+q(2))+m3*p3x*a2*cos(q(3)+2*q(2))-
m3*p3y*a2*sin(q(3)+2*q(2))-
m3*p3x*p3y*sin(2*q(3)+2*q(2))+2*m3*p3x*a1*cos(q(3)+q(2))+1/2*m3*p3x^2*cos(2*
q(3)+2*q(2))+1/2*m3*a2^2*cos(2*q(2))+1/2*m3*p3y^2+1/2*m3*a2^2+1/2*I421*sin(2
*q(4)+2*q(3)+2*q(2))-
1/2*I411*cos(2*q(4)+2*q(3)+2*q(2))+1/2*I412*sin(2*q(4)+2*q(3)+2*q(2))+1/2*I312*s
in(2*q(3)+2*q(2))+1/2*I221*sin(2*q(2))+1/2*I322*cos(2*q(3)+2*q(2))-
1/2*I211*cos(2*q(2))+1/2*I222*cos(2*q(2))+1/2*I212*sin(2*q(2))-
m2*p2x*p2y*sin(2*q(2))+2*m4*a2*a1*cos(q(2))-
1/2*m4*p4y^2*cos(2*q(4)+2*q(3)+2*q(2))+1/2*m4*p4y^2+m4*a1^2+1/2*I411+1/2*I4
22+1/2*I211+1/2*I222+1/2*m4*p4x^2+1/2*m4*a3^2+1/2*m4*a3^2*cos(2*q(3)+2*q(2
))+1/2*m4*p4x^2*cos(2*q(4)+2*q(3)+2*q(2))-
m4*p4y*a3*sin(q(4))+m4*a3*a2*cos(q(3))+2*m4*a3*a1*cos(q(3)+q(2))+m4*a3*a2*co
s(q(3)+2*q(2))+m4*p4x*a2*cos(q(4)+q(3)+2*q(2))+m4*p4x*a3*cos(q(4)+2*q(3)+2*q(
2))-m4*p4y*a2*sin(q(4)+q(3))+m4*p4x*a3*cos(q(4))+1/2*m4*a2^2*cos(2*q(2))-
```
```

m4*p4x*p4y*sin(2*q(4)+2*q(3)+2*q(2))+m4*p4x*a2*cos(q(4)+q(3))+2*m4*p4x*a1*c
os(q(4)+q(3)+q(2))-m4*p4y*a2*sin(q(4)+q(3)+2*q(2))-
2*m4*p4y*a1*sin(q(4)+q(3)+q(2))-
m4*p4y*a3*sin(q(4)+2*q(3)+2*q(2))+1/2*I321*sin(2*q(3)+2*q(2))+m1*p1x^2+1/2*I3
11+1/2*I322

M(1,2) = .2e-7*cos(q3)+.304834872174*sin(q2+q3+q4)-.250872124292e-
1*cos(q2+q3+q4)-.4e-8*sin(2*q1)-.27e-8*cos(2*q1)+.4e-8*sin(2*q2+2*q3)+.520e-7-
.3e-7*cos(2*q3+2*q1+2*q2)+.1e-6*cos(2*q1-2*q2)-.4e-8*sin(2*q2)-.250872124292e-
1*cos(1.*q4+1.*q3+1.*q2)+.304834872174*sin(1.*q4+1.*q3+1.*q2)-.1e-
6*cos(2*q1+2*q2)+.87e-10*sin(2*q1+q4+q3+q2)+.2e-7*cos(q3+2*q2)

M(1,3) = .304834872174*sin(q2+q3+q4)-.250872124292e-1*cos(q2+q3+q4)+.4e-
8*sin(2*q1)+.94e-8*cos(2*q1)-.47e-8*cos(2*q2+2*q3)-.2e-8*sin(2*q2+2*q3)-
.250872124292e-1*cos(1.*q4+1.*q3+1.*q2)+.304834872174*sin(1.*q4+1.*q3+1.*q2)

M(1,4) = I423*cos(q(4)+q(3)+q(2))+I413*sin(q(4)+q(3)+q(2))-
m4*p4z*sin(q(4)+q(3)+q(2))*p4x-m4*p4z*cos(q(4)+q(3)+q(2))*p4y

M(2,1) = -m3*p3z*sin(q(3)+q(2))*p3x-
m3*p3z*cos(q(3)+q(2))*p3y+cos(q(2))*I232+I431*sin(q(4)+q(3)+q(2))+sin(q(2))*I231-
m2*p2z*sin(q(2))*p2x-m2*p2z*cos(q(2))*p2y+I432*cos(q(4)+q(3)+q(2))-
m4*p4z*cos(q(4)+q(3)+q(2))*p4y+I331*sin(q(3)+q(2))+I332*cos(q(3)+q(2))-
m3*p3z*sin(q(2))*a2-m4*p4z*sin(q(3)+q(2))*a3-m4*p4z*sin(q(4)+q(3)+q(2))*p4x-
m4*p4z*sin(q(2))*a2

M(2,2) = m2*p2y^2+m2*p2x^2+m3*a2^2+m3*p3y^2+m3*p3x^2+I433+I233-
2*m3*p3y*a2*sin(q(3))+2*m3*p3x*a2*cos(q(3))+I333+m4*a2^2+m4*p4x^2+m4*a3^2
+m4*p4y^2+2*m4*a3*a2*cos(q(3))-
2*m4*p4y*a3*sin(q(4))+2*m4*p4x*a3*cos(q(4))+2*m4*p4x*a2*cos(q(4)+q(3))-
2*m4*p4y*a2*sin(q(4)+q(3))

M(2,3) = m3*p3y^2+m3*a2*p3x*cos(q(3))+I433+m4*a2*p4x*cos(q(4)+q(3))-
2*m4*p4y*a3*sin(q(4))+2*m4*p4x*a3*cos(q(4))+m4*p4y^2+m4*a3^2+m4*p4x^2-
m4*a2*p4y*sin(q(4)+q(3))+m4*a2*a3*cos(q(3))+I333+m3*p3x^2-
m3*a2*p3y*sin(q(3))

M(2,4) = m4*p4x^2+I433+m4*a3*p4x*cos(q(4))-
m4*a3*p4y*sin(q(4))+m4*p4y^2+m4*a2*p4x*cos(q(4)+q(3))-
m4*a2*p4y*sin(q(4)+q(3))

M(3,1) = I431*sin(q(4)+q(3)+q(2))+I432*cos(q(4)+q(3)+q(2))-
m4*p4z*sin(q(3)+q(2))*a3+I332*cos(q(3)+q(2))-m4*p4z*cos(q(4)+q(3)+q(2))*p4y-
m4*p4z*sin(q(4)+q(3)+q(2))*p4x-m3*p3z*sin(q(3)+q(2))*p3x-
m3*p3z*cos(q(3)+q(2))*p3y+I331*sin(q(3)+q(2))

M(3,2) = -
m3*a2*p3y*sin(q(3))+m3*p3x^2+m3*p3y^2+I433+I333+m4*p4x^2+m3*a2*p3x*cos(q(3))-2*m4*p4y*a3*sin(q(4))+m4*p4y^2+m4*a3^2+2*m4*p4x*a3*cos(q(4))-m4*a2*p4y*sin(q(4)+q(3))+m4*a2*a3*cos(q(3))+m4*a2*p4x*cos(q(4)+q(3))

M(3,3) = m4*p4y^2+m4*p4x^2+m4*a3^2+2*m4*p4x*a3*cos(q(4))-2*m4*p4y*a3*sin(q(4))+I433+I333+m3*p3x^2+m3*p3y^2

M(3,4) = m4*a3*p4x*cos(q(4))-m4*a3*p4y*sin(q(4))+I433+m4*p4x^2+m4*p4y^2

M(4,1) = -m4*p4z*sin(q(4)+q(3)+q(2))*p4x-m4*p4z*cos(q(4)+q(3)+q(2))*p4y+I432*cos(q(4)+q(3)+q(2))+I431*sin(q(4)+q(3)+q(2))

M(4,2) = m4*p4x^2+I433-m4*a3*p4y*sin(q(4))+m4*p4y^2+m4*a2*p4x*cos(q(4)+q(3))+m4*a3*p4x*cos(q(4))-m4*a2*p4y*sin(q(4)+q(3))

M(4,3) = m4*p4y^2+m4*p4x^2+m4*a3*p4x*cos(q(4))-m4*a3*p4y*sin(q(4))+I433

M(4,4) = m4*p4y^2+I433+m4*p4x^2

V(1) = (-2*m3*p3x*a1*sin(q(3)+q(2))-2*m4*a2*a1*sin(q(2))+I421*cos(2*q(4)+2*q(3)+2*q(2))+I411*sin(2*q(4)+2*q(3)+2*q(2))+I412*cos(2*q(4)+2*q(3)+2*q(2))-I422*sin(2*q(4)+2*q(3)+2*q(2))-2*m4*p4x*a2*sin(q(4)+q(3)+2*q(2))-2*m2*cos(q(2))*p2y*a1-2*m3*sin(q(2))*a2*a1-2*m3*p3y*a2*cos(q(3)+2*q(2))-2*m3*p3x*a2*sin(q(3)+2*q(2))-2*m3*p3x*p3y*cos(2*q(3)+2*q(2))-2*m2*p2x*p2y*cos(2*q(2))-2*m3*p3y*a1*cos(q(3)+q(2))-2*m4*p4x*a1*sin(q(4)+q(3)+q(2))-2*m4*p4y*a1*cos(q(4)+q(3)+q(2))-2*m4*a3*a1*sin(q(3)+q(2))-2*m4*p4x*a3*sin(q(4)+2*q(3)+2*q(2))-2*m2*sin(q(2))*p2x*a1-2*m4*a3*a2*sin(q(3)+2*q(2))-2*m4*p4x*p4y*cos(2*q(4)+2*q(3)+2*q(2))-2*m4*p4y*a2*cos(q(4)+q(3)+2*q(2))-2*m4*p4y*a3*cos(q(4)+2*q(3)+2*q(2))+I312*cos(2*q(3)+2*q(2))+I221*cos(2*q(2))-I322*sin(2*q(3)+2*q(2))+I211*sin(2*q(2))-I222*sin(2*q(2))+I212*cos(2*q(2))+I311*sin(2*q(3)+2*q(2))-m4*a3^2*sin(2*q(3)+2*q(2))-m4*p4x^2*sin(2*q(4)+2*q(3)+2*q(2))-m4*a2^2*sin(2*q(2))+m4*p4y^2*sin(2*q(4)+2*q(3)+2*q(2))-m3*a2^2*sin(2*q(2))-m3*p3x^2*sin(2*q(3)+2*q(2))+I321*cos(2*q(3)+2*q(2))+m3*p3y^2*sin(2*q(3)+2*q(2))-m2*p2x^2*sin(2*q(2))+m2*p2y^2*sin(2*q(2)))*qd(1)*qd(2)+(-m4*p4x*a2*sin(q(4)+q(3))-2*m3*p3x*a1*sin(q(3)+q(2))+I421*cos(2*q(4)+2*q(3)+2*q(2))+I411*sin(2*q(4)+2*q(3)+2*q(2))+I412*cos(2*q(4)+2*q(3)+2*q(2))-I422*sin(2*q(4)+2*q(3)+2*q(2))-m4*p4x*a2*sin(q(4)+q(3)+2*q(2))-m3*p3y*a2*cos(q(3)+2*q(2))-m3*p3x*a2*sin(q(3)+2*q(2))-2*m3*p3x*p3y*cos(2*q(3)+2*q(2))-m3*p3y*a2*cos(q(3))-2*m3*p3y*a1*cos(q(3)+q(2))-2*m4*p4x*a1*sin(q(4)+q(3)+q(2))-2*m4*p4y*a1*cos(q(4)+q(3)+q(2))-

2*m4*a3*a1*sin(q(3)+q(2))-2*m4*p4x*a3*sin(q(4)+2*q(3)+2*q(2))-
m4*a3*a2*sin(q(3)+2*q(2))-2*m4*p4x*p4y*cos(2*q(4)+2*q(3)+2*q(2))-
m4*p4y*a2*cos(q(4)+q(3)+2*q(2))-
2*m4*p4y*a3*cos(q(4)+2*q(3)+2*q(2))+I312*cos(2*q(3)+2*q(2))-
I322*sin(2*q(3)+2*q(2))-m4*p4y*a2*cos(q(4)+q(3))+I311*sin(2*q(3)+2*q(2))-
m4*a3^2*sin(2*q(3)+2*q(2))-m4*p4x^2*sin(2*q(4)+2*q(3)+2*q(2))-
m3*p3x*a2*sin(q(3))+m4*p4y^2*sin(2*q(4)+2*q(3)+2*q(2))-
m3*p3x^2*sin(2*q(3)+2*q(2))+I321*cos(2*q(3)+2*q(2))+m3*p3y^2*sin(2*q(3)+2*q(2)
)-m4*a3*a2*sin(q(3)))*qd(1)*qd(3)+(-
m4*p4x^2*sin(2*q(4)+2*q(3)+2*q(2))+m4*p4y^2*sin(2*q(4)+2*q(3)+2*q(2))-
I422*sin(2*q(4)+2*q(3)+2*q(2))+I421*cos(2*q(4)+2*q(3)+2*q(2))+I411*sin(2*q(4)+2*
q(3)+2*q(2))+I412*cos(2*q(4)+2*q(3)+2*q(2))-m4*p4x*a3*sin(q(4))-
m4*p4y*a2*cos(q(4)+q(3))-m4*p4x*a3*sin(q(4)+2*q(3)+2*q(2))-
m4*p4x*a2*sin(q(4)+q(3)+2*q(2))-m4*p4y*a3*cos(q(4))-
m4*p4y*a3*cos(q(4)+2*q(3)+2*q(2))-m4*p4y*a2*cos(q(4)+q(3)+2*q(2))-
m4*p4x*a2*sin(q(4)+q(3))-2*m4*p4x*p4y*cos(2*q(4)+2*q(3)+2*q(2))-
2*m4*p4y*a1*cos(q(4)+q(3)+q(2))-2*m4*p4x*a1*sin(q(4)+q(3)+q(2)))*qd(1)*qd(4)+(-
m3*p3z*cos(q(3)+q(2))*p3x+m3*p3z*sin(q(3)+q(2))*p3y-m3*p3z*cos(q(2))*a2-
sin(q(3)+q(2))*I323+cos(q(3)+q(2))*I313-
I423*sin(q(4)+q(3)+q(2))+I413*cos(q(4)+q(3)+q(2))-m4*p4z*cos(q(2))*a2-
m2*p2z*cos(q(2))*p2x+m2*p2z*sin(q(2))*p2y+cos(q(2))*I213-sin(q(2))*I223-
m4*p4z*cos(q(4)+q(3)+q(2))*p4x+m4*p4z*sin(q(4)+q(3)+q(2))*p4y-
m4*p4z*cos(q(3)+q(2))*a3)*qd(2)^2+2*(-
m3*p3z*cos(q(3)+q(2))*p3x+m3*p3z*sin(q(3)+q(2))*p3y-
sin(q(3)+q(2))*I323+cos(q(3)+q(2))*I313-
I423*sin(q(4)+q(3)+q(2))+I413*cos(q(4)+q(3)+q(2))-
m4*p4z*cos(q(4)+q(3)+q(2))*p4x+m4*p4z*sin(q(4)+q(3)+q(2))*p4y-
m4*p4z*cos(q(3)+q(2))*a3)*qd(2)*qd(3)+2*(-
I423*sin(q(4)+q(3)+q(2))+I413*cos(q(4)+q(3)+q(2))-
m4*p4z*cos(q(4)+q(3)+q(2))*p4x+m4*p4z*sin(q(4)+q(3)+q(2))*p4y)*qd(2)*qd(4)+(-
m3*p3z*cos(q(3)+q(2))*p3x+m3*p3z*sin(q(3)+q(2))*p3y-
sin(q(3)+q(2))*I323+cos(q(3)+q(2))*I313-
I423*sin(q(4)+q(3)+q(2))+I413*cos(q(4)+q(3)+q(2))-
m4*p4z*cos(q(4)+q(3)+q(2))*p4x+m4*p4z*sin(q(4)+q(3)+q(2))*p4y-
m4*p4z*cos(q(3)+q(2))*a3)*qd(3)^2+2*(-
I423*sin(q(4)+q(3)+q(2))+I413*cos(q(4)+q(3)+q(2))-
m4*p4z*cos(q(4)+q(3)+q(2))*p4x+m4*p4z*sin(q(4)+q(3)+q(2))*p4y)*qd(3)*qd(4)+(-
I423*sin(q(4)+q(3)+q(2))+I413*cos(q(4)+q(3)+q(2))-
m4*p4z*cos(q(4)+q(3)+q(2))*p4x+m4*p4z*sin(q(4)+q(3)+q(2))*p4y)*qd(4)^2

V(2) = (1/2*m3*p3z*cos(q(3)+q(2))*p3x-
1/2*m3*p3z*sin(q(3)+q(2))*p3y+1/2*sin(q(2))*I232-1/2*I431*cos(q(4)+q(3)+q(2))-
1/2*cos(q(2))*I231+1/2*m2*p2z*cos(q(2))*p2x-
1/2*m2*p2z*sin(q(2))*p2y+1/2*I432*sin(q(4)+q(3)+q(2))-
1/2*m4*p4z*sin(q(4)+q(3)+q(2))*p4y-
1/2*I331*cos(q(3)+q(2))+1/2*I332*sin(q(3)+q(2))+1/2*m3*p3z*cos(q(2))*a2+1/2*m4*

p4z*cos(q(3)+q(2))*a3+1/2*m4*p4z*cos(q(4)+q(3)+q(2))*p4x+1/2*m4*p4z*cos(q(2))*
a2)*qd(2)*qd(1)+(-2*m3*p3y*a2*cos(q(3))-2*m3*p3x*a2*sin(q(3))-
2*m4*a3*a2*sin(q(3))-2*m4*p4x*a2*sin(q(4)+q(3))-
2*m4*p4y*a2*cos(q(4)+q(3)))*qd(2)*qd(3)+(-2*m4*p4y*a3*cos(q(4))-
2*m4*p4x*a3*sin(q(4))-2*m4*p4x*a2*sin(q(4)+q(3))-
2*m4*p4y*a2*cos(q(4)+q(3)))*qd(2)*qd(4)+(-
1/2*I431*cos(q(4)+q(3)+q(2))+1/2*I432*sin(q(4)+q(3)+q(2))+1/2*m4*p4z*cos(q(3)+q(
2))*a3+1/2*I332*sin(q(3)+q(2))-
1/2*m4*p4z*sin(q(4)+q(3)+q(2))*p4y+1/2*m4*p4z*cos(q(4)+q(3)+q(2))*p4x+1/2*m3*
p3z*cos(q(3)+q(2))*p3x-1/2*m3*p3z*sin(q(3)+q(2))*p3y-
1/2*I331*cos(q(3)+q(2)))*qd(3)*qd(1)+(-m3*p3x*a2*sin(q(3))-
m4*p4x*a2*sin(q(4)+q(3))-m4*p4y*a2*cos(q(4)+q(3))-m4*a3*a2*sin(q(3))-
m3*p3y*a2*cos(q(3)))*qd(3)^2+(-m4*p4x*a2*sin(q(4)+q(3))-2*m4*p4y*a3*cos(q(4))-
2*m4*p4x*a3*sin(q(4))-
m4*p4y*a2*cos(q(4)+q(3)))*qd(3)*qd(4)+(1/2*m4*p4z*cos(q(4)+q(3)+q(2))*p4x-
1/2*m4*p4z*sin(q(4)+q(3)+q(2))*p4y+1/2*I432*sin(q(4)+q(3)+q(2))-
1/2*I431*cos(q(4)+q(3)+q(2)))*qd(4)*qd(1)+(-m4*p4x*a2*sin(q(4)+q(3))-
m4*p4y*a2*cos(q(4)+q(3)))*qd(4)*qd(3)+(-m4*p4x*a3*sin(q(4))-
m4*p4y*a3*cos(q(4))-m4*p4x*a2*sin(q(4)+q(3))-m4*p4y*a2*cos(q(4)+q(3)))*qd(4)^2

V(3) = (-
1/2*I431*cos(q(4)+q(3)+q(2))+1/2*I432*sin(q(4)+q(3)+q(2))+1/2*m4*p4z*cos(q(3)+q(
2))*a3+1/2*I332*sin(q(3)+q(2))-
1/2*m4*p4z*sin(q(4)+q(3)+q(2))*p4y+1/2*m4*p4z*cos(q(4)+q(3)+q(2))*p4x+1/2*m3*
p3z*cos(q(3)+q(2))*p3x-1/2*m3*p3z*sin(q(3)+q(2))*p3y-
1/2*I331*cos(q(3)+q(2)))*qd(3)*qd(1)+(1/2*m3*p3x*a2*sin(q(3))+1/2*m4*p4x*a2*sin
(q(4)+q(3))+1/2*m4*p4y*a2*cos(q(4)+q(3))+1/2*m4*a3*a2*sin(q(3))+1/2*m3*p3y*a2
*cos(q(3)))*qd(3)*qd(2)+(-2*m4*p4x*a3*sin(q(4))-
2*m4*p4y*a3*cos(q(4)))*qd(3)*qd(4)+(1/2*m4*p4z*cos(q(4)+q(3)+q(2))*p4x-
1/2*m4*p4z*sin(q(4)+q(3)+q(2))*p4y+1/2*I432*sin(q(4)+q(3)+q(2))-
1/2*I431*cos(q(4)+q(3)+q(2)))*qd(4)*qd(1)+(1/2*m4*p4x*a2*sin(q(4)+q(3))+1/2*m4*
p4y*a2*cos(q(4)+q(3)))*qd(4)*qd(2)+(-m4*p4x*a3*sin(q(4))-
m4*p4y*a3*cos(q(4)))*qd(4)^2

V(4) = (1/2*m4*p4z*cos(q(4)+q(3)+q(2))*p4x-
1/2*m4*p4z*sin(q(4)+q(3)+q(2))*p4y+1/2*I432*sin(q(4)+q(3)+q(2))-
1/2*I431*cos(q(4)+q(3)+q(2)))*qd(4)*qd(1)+(1/2*m4*p4y*a3*cos(q(4))+1/2*m4*p4x*
a2*sin(q(4)+q(3))+1/2*m4*p4x*a3*sin(q(4))+1/2*m4*p4y*a2*cos(q(4)+q(3)))*qd(4)*q
d(2)+(1/2*m4*p4x*a3*sin(q(4))+1/2*m4*p4y*a3*cos(q(4)))*qd(4)*qd(3)

G(1) = 0

G(2) = m2*g*cos(q(2))*p2x-m2*g*sin(q(2))*p2y+m3*g*p3x*cos(q(3)+q(2))-
m3*g*p3y*sin(q(3)+q(2))+m3*g*cos(q(2))*a2-
m4*g*p4y*sin(q(4)+q(3)+q(2))+m4*g*a3*cos(q(3)+q(2))+m4*g*cos(q(2))*a2+m4*g*p
4x*cos(q(4)+q(3)+q(2))

G(3) = m3*g*p3x*cos(q(3)+q(2))-
m3*g*p3y*sin(q(3)+q(2))+m4*g*p4x*cos(q(4)+q(3)+q(2))-
m4*g*p4y*sin(q(4)+q(3)+q(2))+m4*g*a3*cos(q(3)+q(2))

G(4) = m4*g*p4x*cos(q(4)+q(3)+q(2))-m4*g*p4y*sin(q(4)+q(3)+q(2))